Microbiology (2008), **154**, 2037–2047 DOI 10.1099/mic.0.2008/017483-0

Two GDP-mannose transporters contribute to hyphal form and cell wall integrity in *Aspergillus nidulans*

Loretta Jackson-Hayes, Terry W. Hill, Darlene M. Loprete, Lauren M. Fay, Barbara S. Gordon, Sonia A. Nkashama, Ravi K. Patel and Caroline V. Sartain

Departments of Chemistry and Biology, Rhodes College, Memphis, TN 38112, USA

Correspondence
Loretta Jackson-Hayes
jacksonhayesl@rhodes.edu

Received 12 February 2008
Revised 21 April 2008
Accepted 30 April 2008

In order to identify novel genes affecting cell wall integrity, we have generated mutant strains of the filamentous fungus *Aspergillus nidulans* that show hypersensitivity to the chitin-binding agent Calcofluor White (CFW). Affected loci are designated *cal* loci. The phenotype of one of these alleles, *call11*, also includes shortened hyphal compartments and increased density of branching in the absence of CFW, as well as reduced staining of cell walls by the lectin FITC–Concanavalin A (ConA), which has strong binding affinity for mannosyl residues. We have identified two *A. nidulans* genes (AN8848.3 and AN9298.3, designated *gmtA* and *gmtB*, respectively) that complement all aspects of the phenotype. Both genes show strong sequence similarity to GDP-mannose transporters (GMTs) of *Saccharomyces* and other yeasts. Sequencing of *gmtA* from the *call11* mutant strain reveals a G to C mutation at position 943, resulting in a predicted alanine to proline substitution at amino acid position 315 within a region that is highly conserved among other fungi. No mutations were observed in the mutant strain's allele of *gmtB*. Meiotic mapping demonstrated a recombination frequency of under 1 % between the *call* locus and the *phenA* locus (located ~9.5 kb from AN8848.3), confirming that *gmtA* and *call* are identical. A GmtA–GFP chimera exhibits a punctate distribution pattern, consistent with that shown by putative Golgi markers in *A. nidulans*. However, this distribution did not overlap with that of the putative Golgi equivalent marker CopA–monomeric red fluorescent protein (mRFP), which may indicate that the physically separated Golgi-equivalent organelles of *A. nidulans* represent physiologically distinct counterparts of the stacked cisternae of plants and animals. These findings demonstrate that *gmtA* and *gmtB* play roles in cell wall metabolism in *A. nidulans* similar to those previously reported for GMTs in yeasts.

INTRODUCTION

Filamentous fungi play important roles in nutrient cycling and industry, and several cause diseases of plants and animals. Increasingly, fungi are seen as major threats to immunosuppressed individuals, such as organ recipients and patients with cancer or HIV (Turner *et al.*, 2006). One of the structures that differentiates a fungus from its host is the chitinous cell wall, which mediates many of the organism's interactions with its environment and regulates cell shape at all stages of development. An improved understanding of the fungal wall and of the processes that determine its integrity would add to our ability to control activities of fungal friends and foes (Maertens & Boogaerts, 2000). In addition to chitin and other polysaccharides, which play principally structural roles, a variety of proteins are also localized within cell walls (De Groot *et al.*, 2005; Bowman & Free, 2006; Lesage & Bussey, 2006; Richard & Plaine, 2007). These play a variety of roles, including cell adhesion (Verstrepen *et al.*, 2004), mediation of iron uptake (Protchenko *et al.*, 2001), cell wall remodelling (reviewed by Lesage & Bussey, 2006), regulation of cell wall porosity (De Nobel *et al.*, 1990), and maintenance of cell wall integrity (van der Vaart *et al.*, 1995).

All cell wall proteins characterized to date are glycoproteins, which have been modified by post-translational addition of mannose and other sugars (De Groot *et al.*,

Abbreviations: CFW, Calcofluor White; ConA, Concanavalin A; ER, endoplasmic reticulum; GMT, GDP-mannose transporter; mRFP, monomeric red fluorescent protein; NST, nucleotide sugar transporter; RFP, red fluorescent protein.

A supplementary figure showing the alignment of amino acid sequences of fungal GDP-mannose transporters is available with the online version of this paper.

2005; Bowman & Free, 2006). All evidence indicates that this process takes place within an endomembrane system (Bourett *et al.*, 2007) that is functionally equivalent to that of higher plants and animals, though a significant structural difference exists in the fungal Golgi apparatus, which consists of unstacked, dispersed cisternae termed 'Golgi equivalents' (Howard, 1981). (For the sake of brevity, this structure will be referred to simply as the 'Golgi' in this paper.) Secreted fungal proteins typically contain evolutionarily conserved *N*-linked oligosaccharides similar to those found in animal glycoproteins (Dean, 1999), and many are also heavily *O*-glycosylated in domains rich in serine and threonine residues (Willer *et al.*, 2005). In fungi, in contrast to mammals, mannosyl residues are the dominant structural component of both classes of oligosaccharide (Mansour & Levitz, 2003). In both classes, glycosylation is initiated in the endoplasmic reticulum (ER), where either a simple (*O*-linked) or complex pre-assembled (*N*-linked) precursor is transferred from a lipid donor to the recipient protein. After transfer of the glycoproteins to the Golgi via regulated vesicular traffic, oligosaccharide modification continues in a multi-step process, dependent upon glycosidases, glycosyltransferases and membrane transporters (Gemmill & Trimble, 1999). The sugar donors in glycosyltransferase reactions are nucleotide sugars. These solutes must be transported from the cytosol into the Golgi lumen by specific nucleotide sugar transporters (NSTs), which are type III transmembrane proteins (Berninsone & Hirschberg, 2000). The best studied of these is the *Saccharomyces cerevisiae* GDP-mannose transporter (GMT) VRG4, which forms autodimers in the functional state (Gao & Dean, 2000).

Because cell wall glycoproteins must transit through and be modified within the endomembrane system, a wide range of intracellular proteins must be expected to play roles in determining wall structure and function (Goto, 2007). Accordingly, critical wall-related and morphogenetic roles have been demonstrated for several proteins involved in vesicular traffic (e.g. Whittaker *et al.*, 1999; Shaw *et al.*, 2002; Shi *et al.*, 2004; Yang *et al.*, 2008) and in the pathways of protein mannosylation (e.g. Shaw & Momany, 2002; Willer *et al.*, 2005; Upadhyay & Shaw, 2006).

Our laboratory is interested in identifying new genes whose activity is important to the integrity of cell walls in filamentous fungi. Mutants with cell wall defects can be identified in a variety of ways; many, for instance, are highly sensitive to the chitin-binding agent Calcofluor White (CFW) (e.g. de Groot *et al.*, 2001; Hill *et al.*, 2006). In this study we report the isolation of one such mutation, *calI11* (for Calcofluor hypersensitivity), whose phenotype also includes shortened hyphal compartments with increased branch density in the absence of CFW stress, as well as reduced wall mannosylation. We demonstrate that the *calI11* mutation lies in an *Aspergillus nidulans* orthologue of the *S. cerevisiae* gene encoding the GMT VRG4 (Gao & Dean, 2000), which we designate *gmtA*. The distribution of the GmtA–GFP chimera is consistent with that of Golgi proteins. We also describe a paralogue of *gmtA*, designated *gmtB*, which can act as an extra-copy suppressor of the *calI11* phenotype. To our knowledge, this is the first study of a GMT in a filamentous fungus.

METHODS

Strains, media and basic culture methods. Strains used in this study are listed in Table 1. Complete medium (CM) consisted of 1 % glucose, 0.2 % peptone, 0.1 % yeast extract, 0.1 % casamino acids, 5 % nitrate salts, 1 % trace elements, 0.1 % vitamin mix, 1.2 mM L-arginine, 10 mM uracil and 5 mM uridine. Vitamin mix and nitrate salts are described in the appendix of Kafer (1977). Trace element solution is described in Hill & Kafer (2001). Minimal medium (MM) consisted of 1 % glucose, 5 % nitrate salts, 1 % trace elements, 0.001 % thiamine hydrochloride and 25 ng biotin ml^{-1}. Solid media contained 1.5 % agar and 50 mg ampicillin ml^{-1}. All cultures were incubated at 30 °C.

Mutagenesis, screening, and Mendelian analyses. Conidia of *A. nidulans* strain A28 were mutagenized to 50 % mortality with 4-nitroquinoline-1-oxide (NQO) as described by Harris *et al.* (1994).

Table 1. *A. nidulans* strains used in this study

Strain	Genotype*
A28†	*pabaA6 biA1*
A498†	*biA1*; *phenA2*
RCH-30‡	*calI11*; *pabaA6 biA1*
GR5†	*pyrG89*; *wA3*; *pyroA4*
R205‡	*calI11*; *pyrG89*; *wA3*; *pyroA4*
R475‡	*calI11*; *gmtA*::Nc*Pyr4*; *pyrG89*; *wA3*; *pyroA4*
R476‡	*calI11*; *gmtB*::Nc*Pyr4*; *pyrG89*; *wA3*; *pyroA4*
A1145†	*pyrG89*; *pyroA4*; *nkuA*::*argB*; *riboB2*; *argB2*
R633‡	*gmtA-GFP*::Af*pyrG*; *pyrG89*; *pyroA4*; *nkuA*::Af*argB*; *riboB2*
R559‡	*gmtA-GFP*::Af*pyrG*; *copA-mRFP*::Af*riboB*; *pyrG89*; *pyroA4*; *nkuA*::Af*argB*; *riboB2*; *argB2*

*Nc, *Neurospora crassa*; Af, *A. fumigatus*.
†Available from Fungal Genetics Stock Center, University of Missouri, Kansas City, MO, USA (McCluskey, 2003).
‡Generated during this study.

Survivors were screened for sensitivity to 10 μg CFW ml^{-1} ('Blankophor BBH', a gift from Bayer Corporation) as described in Hill *et al.* (2006). Strain RCH-30, which exhibited CFW hypersensitivity along with compact colony diameter, was selected for further study and crossed with strain GR5, which has wild-type branching and CFW sensitivity, using standard genetic methods (Kafer, 1977; Kaminskyj, 2000). Analysis of the resulting progeny showed that hypersensitivity and small colony diameter co-segregated in a 1 : 1 ratio, and both traits were recessive in the diploid state. Strain R205 (*pyrG89*; *wA3*; *calI11*; *pyroA4*) used elsewhere in this research was selected from this cross. Diploids constructed between RCH-30 and strains bearing mutations in *cal* loci described previously (*calA–H*, allele numbers *1–10*; Hill *et al.*, 2006) confirmed that the RCH-30 mutation was in an independent locus. For this reason we have designated the allele *calI11*, following the nomenclature recommendations of Clutterbuck & Arst (1995). Following the identification of a base substitution in the mutant strain allele of AN8848.3 (*gmtA*), a sexual cross was performed between *calI11* strain R205 and *phenA2* strain A498 to test for linkage between the two loci. Only 9.5 kb separated *phenA* from AN8848 (according to The *Aspergillus nidulans* Linkage Map; http://www.gla.ac.uk/ibls/molgen/aspergillus/index.html).

Library transformations and identification of complementing genes. Strain R205 was transformed according to Yelton *et al.* (1984) using the AMA-*Not*I genomic library (Osherov *et al.*, 2000). Transformants were selected for restoration of pyrimidine prototrophy on minimal medium containing 1.1 M sorbitol. Conidia from transformed colonies were tested for restoration of wild-type colony morphology and for resistance to CFW, and two complemented strains (R205-XF1 and R205-XF2) were selected for further study. Genomic DNA was isolated from each strain, and plasmids were recovered by transforming competent *Escherichia coli*. Two recovered plasmids (designated pR205-XF1 and pR205-XF2) complemented the *calI11* phenotype upon retransformation of strain R205. The genomic inserts of both plasmids were end-sequenced using vector-specific primers, and the resulting end sequences were compared with the Broad Institute *Aspergillus nidulans* sequenced DNA database (Aspergillus Sequencing Project, Broad Institute of MIT and Harvard; Galagan *et al.*, 2005) to determine the intervening wild-type genomic sequences. One autocalled gene (AN8848.3) was represented in the genomic insert of pR205-XF1, and two (AN9298.3 and AN9299.3) in the insert of pR205-XF2. TBLASTN (http://www.ncbi.nlm.nih.gov/blast/Blast.cgi) was used to search NCBI databases for sequences showing homology to AN8848.3 (*gmtA*) and AN9298.3 (*gmtB*), and alignments with selected sequences were performed using CLUSTAL W (European Bioinformatics Institute; http://www.ebi.ac.uk/clustalw/).

Cloning of AN8848.3 (*gmtA*), AN9298.3 (*gmtB*) and AN9299.3. Candidate genes were PCR-amplified from A28 genomic DNA with an additional 600–1000 bp of upstream sequence and 100 bp of downstream sequence, using *Pfu* Turbo polymerase (Stratagene) and gene-specific primers (Table 2). PCR products were purified using the Qiagen PCR purification kit, and gel pieces were purified using the Qiagen QIAquick Gel Extraction kit. The cleaned PCR products were ligated into the pRG3-AMA1-*Not*I plasmid (Fungal Genetics Stock Center, University of Missouri, Kansas City, MO), using the Quick Ligation kit (New England Biolabs). The constructs containing wild-type *gmtA*, *gmtB* and AN9299.3 were designated pLJH131, pLJH133 and pLJH134, respectively. Protoplasts from strain R205 were

Table 2. Primers used in this study

Primer	Sequence*	Restriction site
Cloning primers		
AN9299.3 5′	ATAGCATGCTAACTTGAGCCGTGAAGTGAG	*Sph*I
AN9299.3 3′	ATAGCATGCACAGCCAGTCCAGACCAAC	*Sph*I
gmtA 5′	ATAGCGGCCGCTCCAGTCCAGCAGTTCCC	*Not*I
gmtA 3′	ATAGCGGCCGCAGCCACTCCCGCGATAAC	*Not*I
gmtB 5′	ATAGCGGCCGCAATCTGGTTTAGTCGACTCT GCA	*Not*I
gmtB 3′	ATAGCGGCCGCAGATACGTCTATAGCCGCCTTTG	*Not*I
GFP/mRFP primers		
gmtA P1 (forward)	GTGTGTATCATTGCAATCCAATTG	
gmtA P3 (reverse)	AGCGCCTGCACCAGCTCCCGAGCGCAGCGAATC	
gmtA P4 (forward)	GTGCCTCCTCTCAGACAGAGATTCAGCTATTTTGCGACTG	
gmtA P6 (reverse)	CTGCTTAGGGACACGAAGACTAG	
gmtA nested (forward)	TTACTAGTGGCTCGGAAGTGTGCGT	*Spe*I
gmtA nested (reverse)	TTATGCATCGGCACAATTGGCCTTG	*Nsi*I
GA5-GFP-Af-*pyrG* 5′	GGAGCTGGTGCAGCG	
GA5-GFP-Af-*pyrG* 3′	CTGTCTGAGAGGAGGCACTGA	
copA P1	CAAGCGAAGCCTTGAGCTT	
copA P3	AGCGCCTGCACCAGCTCCGAGTTGGCTAGGGACATACAAC	
copA P4	TCGCGGACGTGGTCGAGGTCCCCTGAC GACGTGTGAT	
copA P6	TTTCCGGAACTGGATGGC	
copA nested (forward)	GCCTACTTCACTATTCCCAAGCT	
copA nested (reverse)	GAGAAGTGAGTTTGGGAATTGG	
Af-*riboB* 5′	TTTCTAGAATCACATGGGATTAAAATATGGTGT	*Xba*I
Af-*riboB* 3′	TTTCTAGATTACATGAGTGTGACGAGCATACA	*Xba*I
GA5-mRFP-Af-*riboB* 5′	GGAGCTGGTGCAGGCG	
GA5-mRFP-Af-*riboB* 3′	TTACATGAGTGTGACGAGCATACA	

*The underlined sequence corresponds to the indicated restriction site.

transformed separately with the different constructs, and transformants were tested for complementation of the *calI11* phenotype, confirming that the complementing sequences are wild-type AN8848.3 (*gmtA*) and AN9298.3 (*gmtB*).

Sequencing the mutant allele. The *gmtA* and *gmtB* alleles of the *calI11* mutant strain were amplified from R205 genomic DNA using the same primers used in the preceding section and *Pfu* Turbo. Two separate PCR reactions were run for each gene, and products from each reaction were cloned into pGEM-5Zf(+) (Promega) before transformation of competent *E. coli*. Two clones from each PCR reaction were selected for sequencing using overlapping primer sets (not listed), giving at least twofold coverage of each sequence. The respective sequences were aligned to the wild-type (strain A4) genomic DNA sequence in the Broad Institute database and to our own sequences of the identical region of strain GR5 (parent strain of strain R205) with CLUSTAL W in order to identify the genetic lesion in *gmtA*.

Expression of GFP and red fluorescent protein (RFP) chimeras. We have not been successful in generating a stable transformant that expresses a GmtB–GFP chimera. A *gmtA–GFP* expression construct was generated by fusion PCR (Szewczyk *et al.*, 2006). An initial round of PCR reactions was performed to amplify the 1 kb 5′- and 3′-flanking regions of *gmtA* using *Pfu* Turbo and genomic DNA of strain A1145 (Nayak *et al.*, 2006) as a template. Primers used in amplifying the 5′-flanking regions were designed to omit the stop codons from the expression constructs (Table 2). Also included in the initial round of PCR reactions was a reaction amplifying the *GA5-GFP*-Af-*pyrG* cassette using plasmid pFNO3 (Yang *et al.*, 2004; Fungal Genetics Stock Center) as a template. Each of the three PCR products was run on a 0.65 % agarose gel, and the appropriately sized fragments were excised and gel-purified as described above. Fusion PCR reactions to generate the linear *gmtA-GFP*-Af-*pyrG* expression construct contained 100 ng each of 5′- and 3′-flanking regions and *GA5-GFP*-Af-*pyrG* cassette. The fusion products were run on 0.65 % agarose gels, and the linear 4.6 kb *gmtA-GFP*-Af-*pyrG* construct was excised and gel-purified using the QIAquick Gel Extraction kit. The *nkuA* deletion strain A1145 was transformed according to Osmani *et al.* (2006) to create strain R633, and transformants were selected for conversion to pyrimidine prototrophy on MM plates supplemented with 1.1 M sorbitol, 0.05 μg pyridoxine ml^{-1} and 0.1 μg riboflavin ml^{-1}.

In order to create strains that expressed GmtA–GFP along with CopA–monomeric RFP (mRFP), a *GA5–mRFP* cassette containing the *riboB* gene from *Aspergillus fumigatus* was constructed. The *riboB* gene (Afu1g13300), along with 500 bp of 5′-flanking and 100 bp of 3′-flanking sequence, was PCR-amplified using primers that added *Xba*I sites at the 5′ and 3′ ends (Table 2) using *A. fumigatus* (strain A1100) genomic DNA as a template. Plasmid pXDRFP4 (Yang *et al.*, 2004; Fungal Genetics Stock Center) was digested with *Xba*I (which digests within the sequence between the mRFP sequence and the *pyrG* sequence, and in the PCR-BluntII-TOPO multi-cloning site) to remove *pyrG*, and *Xba*I-treated *riboB* was cloned into *Xba*I-digested pXDRFP4. The expression construct (CopA–mRFP) was generated in a manner similar to that utilized in creating the *gmtA-GFP*-Af-*pyrG* expression constructs. The initial round of PCR amplified 500 bp of the 5′- and 3′-flanking regions of *CopA* (AN3026.3) and the *GA5-mRFP*-Af-*riboB* cassette. Each of the three products was gel-purified, and 100 ng of each was used in a fusion PCR reaction that produced a linear 3.6 kb *CopA-mRFP*-Af-*riboB* construct. Gel-purified *CopA-mRFP*-Af-*riboB* was used to transform strain R633 (A1145/*gmtA-GFP*) according to Osmani *et al.* (2006), and transformants were selected for conversion to riboflavin prototrophy on MM plates supplemented with 1.1 M sorbitol and 0.05 μg pyridoxine ml^{-1}.

Microscopic methods and morphological characterization of the *calI11* phenotype. All observations were made using an Olympus BX51 epifluorescence microscope, in either fluorescence or transmitted-light mode, equipped with a SPOT RT-SEM digital camera (Diagnostic Instruments). Fluorescence observations employed a ×100 1.35 numerical aperture objective.

Basic morphological observations were made by applying 5 μl drops containing between 500 and 2000 conidia onto agar media and incubating for 15–24 h, after which germlings were covered with liquid medium of matching solute composition and observed under a coverslip. Fluorescence observations were made using liquid-grown coverslip cultures (Harris *et al.*, 1994). For quantitative assessment of septal distance, hyphal width, nuclear numbers, etc., coverslip cultures were fixed, stained with Hoechst 33258 dye (Sigma) and CFW (to stain nuclei and cell walls, respectively), mounted as described by Harris *et al.* (1994) and observed using the Olympus U-MWU2 filter set. Apical compartments were defined as those distal to the first septum, and apical branches were defined as any branch occurring in this compartment. Intercalary compartments are those other than the terminal compartment. Branch density ('intercalary branch number per 10 μm') was calculated by counting the total number of branches in randomly selected five-compartment hyphal segments (intercalary). Spore body diameters were measured at right angles to the longitudinal axis of the germling. Measurements were made from photographs taken with a ×40 objective and displayed at ×1167 magnification. Statistical differences between populations (mutant vs wild-type vs complemented) were determined using two-tailed *t* tests at the 0.05 level of significance, based on the observation of at least 30 randomly selected germlings for each condition.

For staining with FITC–Concanavalin A (FITC–ConA; Sigma), coverslip cultures were washed for 1 min in deionized water, then incubated in 200 μl drops of 250 μg aqueous FITC–ConA ml^{-1} for 30 min at room temperature, followed by a brief water rinse and immediate observation using the Olympus U-WMB2 filter set. Mixed cultures (mutant plus wild-type) were employed to ensure that identical conditions of illumination and photographic exposure were used for comparisons of staining intensity. For observation of cells expressing GFP or mRFP chimeras, coverslips with attached germlings were either transferred directly to slides and observed without fixation, or alternatively they were first fixed for 30 min at room temperature in PIPES-buffered formaldehyde (Kaminskyj, 2000). The U-MWB2 filter set was used for observation of the GFP signal, and the U-MWG2 filter set was used for mRFP. For simultaneous imaging of ER and Gmt–GFP, coverslip-grown germlings of strain R633 were incubated in 200 μl drops of 10 μM ER-Tracker Blue-White DPX (Molecular Probes) in growth medium for 30 min, followed by 30 min in dye-free medium and immediate observation using the U-MWU2 filter set. To assess potential colocalization of differently coloured signals (GFP vs ER-Tracker or GFP vs mRFP), separate channels were first imaged in grayscale, then converted to complementary pseudocolours, and finally merged in RGB mode using Adobe PhotoShop software.

RESULTS

Characterization of *calI11* phenotype

The *calI11* mutant strain was selected principally on the basis of its hypersensitivity to CFW. The strain's complete inability to tolerate exposure to CFW at tested levels (Fig. 1) was comparable to the most extreme sensitivity shown by *cal* mutant strains reported in previous studies (Hill *et al.*, 2006). In addition, *calI11* mutants exhibited severe morphological defects, demonstrated in Fig. 2(a–e) and Table 3, in which intercalary compartments were greatly

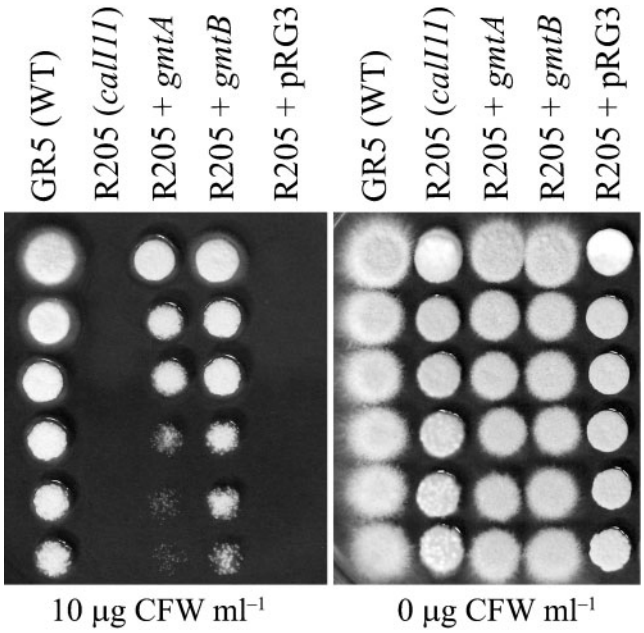

Fig. 1. Sensitivities of mutant, wild-type and transformed strains to CFW. Colonies were grown for 2 days at 30 °C on CM plus pyrimidines, containing either 10 or 0 μg CFW ml^{-1}. Each vertical column is a twofold dilution series, beginning with (top) 10 000 spores in 5 μl. R205 + *gmtA* has been transformed with plasmid pLJH131. R205 + *gmtB* has been transformed with plasmid pLJH133. R205 + pRG3 has been transformed with the empty pRG3 vector (control).

shortened, with a comparable increase in branch density. Septum-to-septum distance was reduced to about 44 % of that of the wild-type. The length of apical compartments was also greatly reduced (to ~22 % of the wild-type length), and all apical compartments contained hyphal branches, compared with just 5 % apical branching frequency in the wild-type. Hyphal width was irregular compared with the wild-type and was significantly increased (~1.3-fold that of wild-type), as was the degree of swelling of spores during germination. (The ~1.8-fold increase in diameter over wild-type equals an approximately sixfold increase in volume.) Many cells bore prominent vacuoles (Fig. 2b). These cellular defects were reflected in a greatly reduced colony size (Fig. 2f). These defects were not remedied by growth with high osmoticum or by media containing elevated levels of mannose.

Complementation of *calI11*

Transformation of the *calI11* mutant strain R205 with an *A. nidulans* high copy plasmid genomic library yielded two strains showing wild-type colony morphology (see Methods), from which two complementing plasmids were recovered: one containing the predicted gene AN8848.3 (1312 bp), and a second containing predicted genes AN9298.3 (927 bp) and AN9299.3 (837 bp). Retransformation with each of the three separately cloned ORFs (including ~600–1000 bp upstream 'promoter' sequence) demonstrated that the complementing genes were AN8848.3 and AN9298.3 (Fig. 1, Table 3). All morphological aspects of the complemented phenotype were restored to essentially wild-type levels, with the exception of the frequency of branching in apical compartments, which was partially, but still significantly, restored (Table 3). Resistance to CFW was restored to nearly, though not fully, wild-type levels (Fig. 1).

A translated BLAST search revealed that the closest homologues of AN8848.3 and AN9298.3 were yeast GMTs (Supplementary Fig. S1; Fig. 3). To reflect this homology, we have assigned the functional gene names *gmtA* and *gmtB*, respectively. AN8848.3 is predicted to encode a 380 aa protein with ~50 % identity and 55 % similarity to *S. cerevisiae* VRG4, while AN9298.3 encodes a predicted 271 aa product with ~43 % identity and 50 % similarity to VRG4 (see Supplementary Fig. S1). GmtA and GmtB share 41 % identity and 58 % similarity. Each of the two gene products is predicted to be a multipass transmembrane protein (SOSUI Engine ver. 1.11; http://bp.nuap.nagoya-u.ac.jp/sosui/).

Identification of the *calI11* mutation

Sequence analysis of AN9298.3 (*gmtB*) copied from R205 genomic DNA revealed no genetic lesion. However, AN8848.3 (*gmtA*) from the same source contained a G to C mutation at base 943, which was predicted to cause an A315P amino acid substitution in predicted exon 4 (Fig. 3). This region is highly conserved in yeasts and filamentous fungi (Fig. 3; Gao & Dean, 2000). A cloned *gmtA* allele containing this same G to C substitution failed to complement the *calI11* phenotype when transformed into strain R205 (data not shown). Further confirmation that *calI* is *gmtA* was obtained from the results of a sexual cross between strains R205 (*calI11*) and strain A498, containing the *phenA2* allele, which is separated from the AN8848.3 locus on chromosome III by ~9.5 kb. Out of 117 progeny tested, only one showed a recombinant phenotype, indicating an exceptionally tight degree of linkage (less than 1 cM map distance).

Mannose deficiency in *calI11* cell walls

In light of the fact that the closest homologues of *gmtA* are transporters of GDP-mannose, we explored the possibility that the *calI11* mutation might cause a detectable reduction in mannosylation of cell wall constituents. Fig. 4 shows a co-culture of strains GR5 and R205 treated with the mannose-binding lectin FITC–ConA, and demonstrates a marked reduction in staining of the mutant cell walls compared with those of wild-type (longer, thinner hyphae in Fig. 4). Mutants complemented with constructs containing either *gmtA* or *gmtB* were restored to wild-type levels of ConA staining (data not shown).

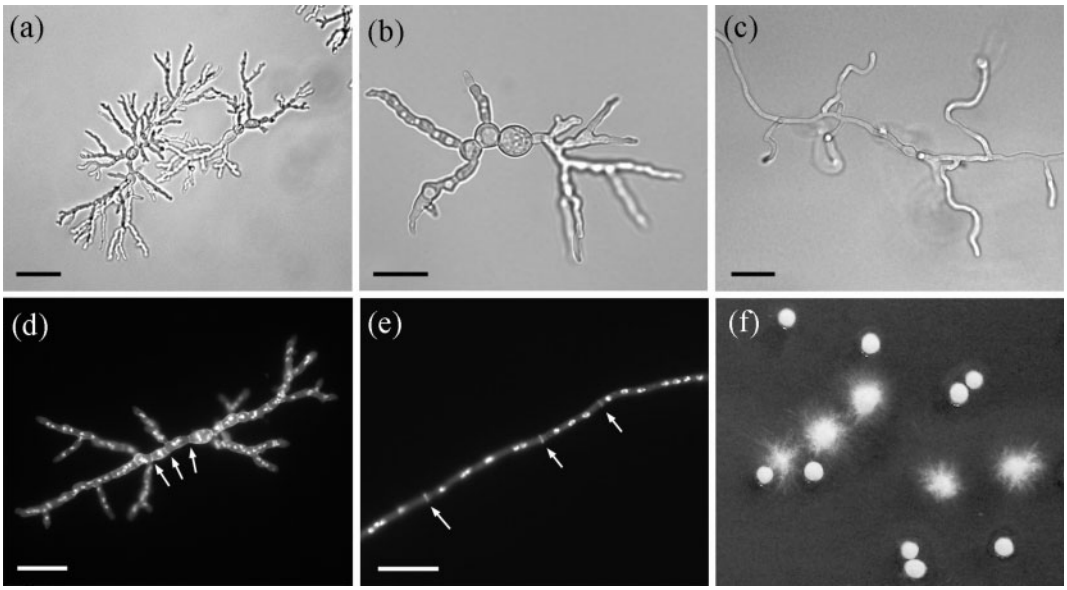

Fig. 2. Effects of *calI11* mutation on cell and colony morphology. (a, b) Transmitted light images of germlings of *calI11* mutant strain R205 at two different magnifications (~24 h old and ~16 h old, respectively) showing hyperbranched, contorted growth form and excessive swelling of the spore body. (c) Transmitted light image of germling of strain GR5 (wild-type morphology) at ~10 h. (d, e) Fluorescence images of strains R205 and GR5, respectively, stained to show nuclei and septa (examples indicated by arrows) using Hoechst 33258 and CFW. (f) Comparison of the tight colony morphology of 2-day-old spore-grown colonies of mutant strain R205 with that of wild-type strain GR5. Bars, 25 μm, except (a),100 μm.

Cellular localization of GmtA

Transformation of mutant strain R205 with a plasmid expressing a C-terminal GFP-labelled wild-type copy of AN8848.3 complemented the *calI11* phenotype, demonstrating the functionality of the GmtA–GFP hybrid protein (data not shown). GmtA–GFP displayed a punctate pattern of fluorescence (Fig. 5a), consistent with those observed in other studies using putative Golgi markers, and markedly different from that shown by the ER-specific dye ER-Tracker (Fig. 5b). Occasional ring-shaped profiles were also observed (Fig. 5b). We studied GmtA localization further by comparing the fluorescence pattern with that of a putative Golgi-localized protein, CopA (Breakspear *et al.*, 2007), which displayed a punctate pattern of fluorescence similar to that observed with GmtA (Fig. 5c, d). Initial observations made with live cells indicated that the two proteins did not colocalize. However, the mobility of both signals was high enough to allow for some organelles to shift position while switching filters, so the observations were repeated using fixed cells (Fig. 5c, d). These observations confirmed that the two signals were in different compartments, with little indication of overlap. CopA distribution was highest within ~20 μm of the

Table 3. Quantitative morphological measurements of *calI11* mutant, wild-type and complemented strains

Only population means are reported (omitting measures of dispersion) for clarity of presentation. In each column, values with the same superscript letter are not significantly different.

Strain*	Intercalary compartment length (μm)	Intercalary compartment width (μm)	Number of intercalary branches per 10 μm	Apical compartment length (μm)	Apical branches (%)	Spore body diameter (μm)
GR5	32.4[a]	3.47[a]	0.35[a]	236[a]	5[a]	5.37[a]
R205	14.3[b]	4.43[b]	1.31[b]	51[b]	100[b]	9.43[b]
GST	14.3[b]	4.06[b]	1.25[b]	48[b]	100[b]	8.88[b]
gmtA	34.0[a]	3.46[a]	0.44[ac]	188[a]	59[c]	5.54[a]
gmtB	34.3[a]	3.28[a]	0.53[c]	205[a]	56[c]	5.34[a]

*GR5, wild-type; R205, *calI11* mutant; GST, R205 transformed with the non-complementing *A. nidulans* gene AN9299.3 (control) in plasmid pLJH134; *gmtA*, R205 transformed with plasmid pLJH131; *gmtB*, R205 transformed with plasmid pLJH133.

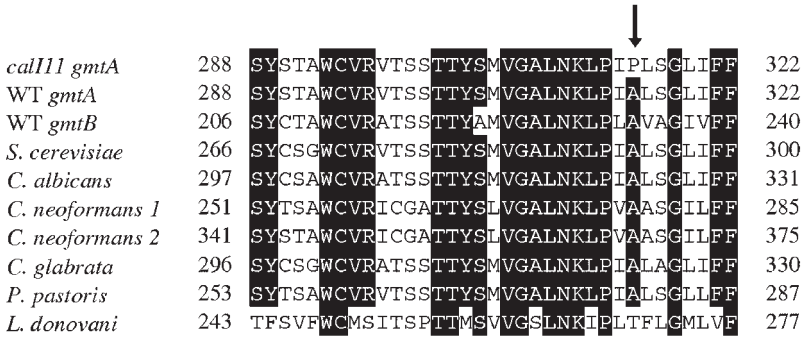

Fig. 3. Location of amino acid substitution in *calI11*. CLUSTAL W alignment of the 'GALNK' motifs of GMTs from several fungal species plus the protozoan parasite *Leishmania donovani*. These are NSTs for which experimental evidence exists to support substrate specificity for GDP-mannose. Conserved amino acids are indicated by shaded characters. The alanine to proline substitution in the *calI11* mutant is indicated by an arrow.

hyphal apex, while GmtA distribution was higher in more basal regions (Fig. 5d).

DISCUSSION

The most distinctive aspects of the *calI11* phenotype are its extreme sensitivity to CFW, its widened stubby hyphal segments, and the increased frequency of branching, including branching in apical compartments. CFW hypersensitivity is well established as an indicator of defects in cell wall integrity (de Groot *et al.*, 2001; Hill *et al.*, 2006), and studies with cell wall mutants and gene deletions have demonstrated an increase in branch density as a result of some wall defects (e.g. Ichinomiya *et al.*, 2002; Mellado *et al.*, 2003). Wild-type *A. nidulans* hyphae generally have few or no branches in the apical compartment and one or fewer branches per intercalary compartment (Turner & Harris, 1999). Hyperbranching mutants tend to have closely spaced septa and wider hyphae, as seen in *calI11*, which leads to the proposal that the number of branches per unit of volume remains about the same in both wild-type and hyperbranching mutants (Turner & Harris, 1999). Since the widths of hyphal compartments in *calI11* are highly irregular, no volumetric calculations were attempted; however, the combination of increased width and decreased length is consistent with the view that compartment volumes are not greatly changed. If, in fact, compartment length changes to keep pace with changes in diameter, then some aspects of hyperbranching may result from changes in determinants of cell polarity at the hyphal tip (Harris *et al.*, 2005), which are ultimately responsible for establishing cell diameter.

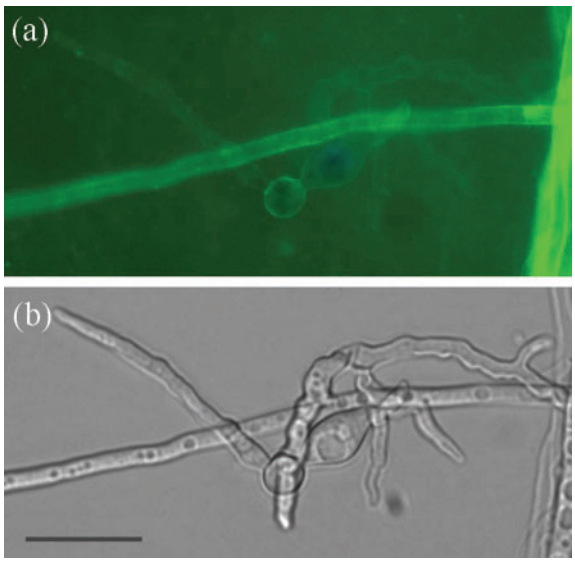

Fig. 4. Differential staining of cell walls of *calI11* mutant and wild-type hyphae by FITC–ConA. (a) Fluorescence image of a mixed culture containing cells of *calI11* mutant strain R205 and wild-type strain GR5. (b) Transmitted light image of the same field. A single wild-type hypha crosses the field horizontally, intersecting with a weakly stained mutant germling. Bar, 25 μm.

The results of this investigation strongly support the conclusion that the defective gene in the *calI11* mutation is a GMT located in a compartment of the Golgi which functions in mannosylation of hyphal wall constituents. All aspects of the *calI11* phenotype are complemented by the wild-type allele of gene AN8848.3, whose closest homologues are fungal GMTs. Meiotic mapping demonstrates that the *calI11* mutant allele resides in the region of chromosome III where AN8848.3 is located, and the AN8848.3 allele of the mutant strain contains a point mutation which renders that allele unable to complement *calI11* when introduced into the pRG3 plasmid. Although substrate specificity among NSTs cannot be predicted from sequence similarity (Berninsone & Hirschberg, 2000), the greatly reduced staining of *calI11*-strain cell walls by the lectin ConA, which has strong binding affinity for mannosyl residues (Baenziger & Fiete, 1979), indirectly supports a defect in mannosylation.

We conclude that AN9298.3 (*gmtB*) represents a second GMT in the *A. nidulans* genome, based upon its sequence homology and its capacity to complement the defect in *gmtA* when overexpressed. The complementing ability of introduced NSTs can be used as a functional demonstration of transporter substrate specificity (Berninsone & Hirschberg, 2000; Cottrell *et al.*, 2007). Whether *gmtB* functions in concert with *gmtA*, or instead performs independent functions in different compartments or at

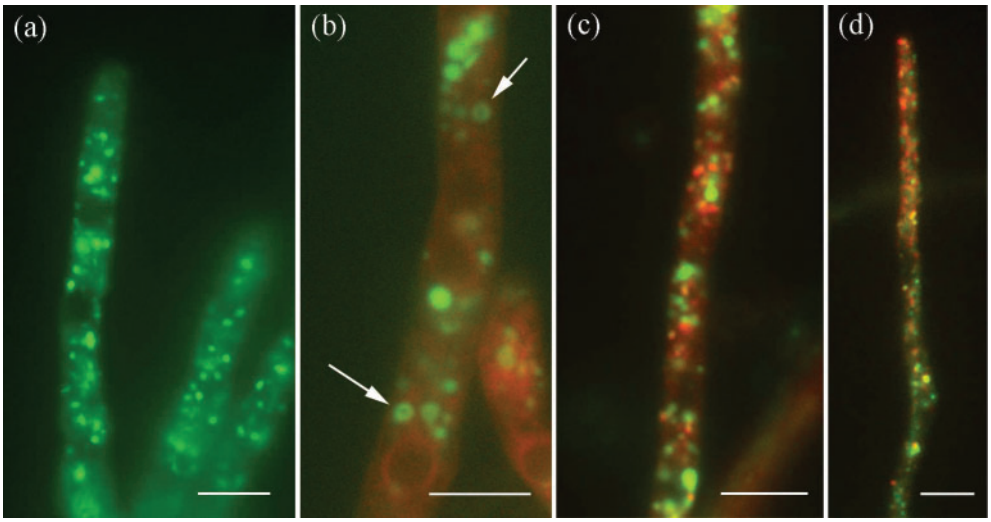

Fig. 5. Subcellular localization of GmtA, ER and CopA. (a) Distribution of GmtA–GFP in living hyphal apices of strain R633. (b) Merged image of strain R633 stained with the ER-specific vital dye ER-Tracker (pseudo-coloured in red), demonstrating the separate localization of ER and GmtA–GFP. Arrows indicate ring-shaped localizations of GmtA–GFP. (c) Merged image of a fixed hypha of strain R559, expressing CopA–mRFP (red signal) and GmtA–GFP (green signal). (d) Merged image of a fixed hypha of strain R559, demonstrating the 'tip-high' distribution of CopA–mRFP (red signal) and the less tip-oriented distribution of GmtA–GFP (green signal). Bars, 5 μm.

different developmental stages, will be the object of further studies.

A role for GMTs in hyphal morphogenesis and wall metabolism, as indicated in this study, is consistent with the results of many other studies in both yeasts and filamentous fungi. Defects in cell wall integrity (indicated by hypersensitivity to wall-compromising agents such as CFW and Congo red) and/or morphological defects, consisting usually of impaired establishment or maintenance of polarity, have been tied to defects in all major stages of mannosylation. These include defects in the cytosolic reactions that precede establishment of mannosyl linkages (Smith & Payton, 1994; Upadhyay & Shaw, 2006), defects in ER protein mannosyltransferases (PMTs) (Timpel *et al.*, 1998; Momany *et al.*, 1999; Shaw & Momany, 2002; Oka *et al.*, 2004; Willer *et al.*, 2005), and defects in the early Golgi mannosyltransferase Och1p (Bates *et al.*, 2006). Furthermore, a screen for *S. cerevisiae* strains showing defects in polarity detected mutants in the GMT VRG4 (Mondésert *et al.*, 1997).

In yeast, defects in protein glycosylation activate major components of the cell wall integrity pathway, including protein kinase C and MAP kinase pathways (Cullen *et al.*, 2006). Mannosylation defects could lead to loss of wall integrity (with potential connections to polarity) through a variety of routes. In *S. cerevisiae*, mutations in VRG4 result in defects in both *N*-linked and *O*-linked protein glycosylation, as well as in synthesis of sphingolipids (Dean, 1999). Some 20–30 % of the mass of filamentous fungal walls consists of proteins, virtually all of which possess mannose-rich oligosaccharides (Bowman & Free, 2006). In *Saccharomyces*, deletion of some of these, such as Cwp2p (van der Vaart *et al.*, 1995), results in increased sensitivity to wall-compromising agents such as CFW, Congo red and zymolyase. In addition, two plasma membrane proteins playing 'sensor' roles in the yeast cell wall integrity pathway, Mid2p and Wsc1p, are heavily *O*-glycosylated (Philip & Levin, 2001). The reduction in production of sphingolipids (Dean, 1999) provides a potential direct link between glycosylation and cell polarity, since sphingolipids have been shown to play roles in polarity establishment and maintenance (e.g. Cheng *et al.*, 2001), most likely through their structural roles as components of lipid rafts. Some of the hyphal growth forms observed by Cheng *et al.* (2001) upon repression of sphingolipid synthesis resemble the hyphal growth forms of the *calI11* mutation.

The mutation identified in the *calI11* allele is predicted to cause an amino acid substitution within a region that is highly conserved in fungi. This region, which contains the 'GALNK' motif, has been shown to be required for nucleotide sugar binding (Gao *et al.*, 2001). In *S. cerevisiae* the consensus GALNK motif spans residues 271–292, and the mutation that we identified affects an amino acid lying one residue outside the consensus region at the equivalent of VRG4 amino acid 293. The alanine at this position is conserved in *S. cerevisiae*, *Candida albicans* (Nishikawa *et al.*, 2002), *Cryptococcus neoformans* GMT1 and GMT2 (Cottrell *et al.*, 2007), and *A. nidulans* GmtB. Several *S. cerevisiae* glycosylation mutants have been identified whose mutations occur within the GALNK region, resulting in a defect in transport activity (Gao *et al.*, 2001).

In *S. cerevisiae, Candida albicans* and *Pichia pastoris*, GMTs reside in the Golgi (Dean *et al.*, 1997; Nishikawa *et al.*, 2002; Losev *et al.*, 2006; Arakawa *et al.*, 2006). The punctate distribution pattern displayed by GmtA–GFP in our studies is consistent with the distribution of proven Golgi markers in yeasts (Dean *et al.*, 1997; Gao & Dean, 2000; Abe *et al.*, 2004), and of putative Golgi markers in *A. nidulans* (Breakspear *et al.*, 2007; Hubbard & Kaminskyj, 2008). Of particular interest in this regard is our observation of occasional ring-shaped profiles of GmtA–GFP, which were also observed by Breakspear *et al.* (2007) for the *A. nidulans* α-COP homologue CopA, and which are consistent with the distinctive appearance of filamentous fungal Golgi-equivalent cisternae in ultrastructural studies (Howard, 1981). In *Saccharomyces* and other yeasts, localization of VRG4 to the Golgi depends upon an evolutionarily conserved lysine-rich C-terminal motif (Abe *et al.*, 2004). Such a region is found in GmtA, *Cryptococcus neoformans* GMT1 and GMT2, and *S. cerevisiae* Hvg1, but not in GmtB according to the gene annotation in Version 3 of the Broad Institute *A. nidulans* sequenced DNA database (Supplementary Fig. S1). We have not yet been able to GFP-tag GmtB, to determine its subcellular location.

An unexpected result is the failure of GmtA to co-localize with CopA, the *A. nidulans* homologue of α-COP (Whittaker *et al.*, 1999), which is a component of the seven-subunit coat protein I (COPI) coatomer complex required for retrograde transport between Golgi compartments, and between Golgi and ER in mammalian cells and yeasts (Cosson & Letourneur, 1997). Subunits of the COPI coat have been shown to localize to Golgi membranes in mammals (Griffiths *et al.*, 1995) and *Saccharomyces* (Morin-Ganet *et al.*, 2000). In *S. cerevisiae*, COPI is required for steady-state localization of VRG4 to the Golgi, and VRG4 has been shown to physically interact with the Ret2p component of the COPI coat (Abe *et al.*, 2004) in a manner dependent upon the C-terminal lysine-rich targeting motif of the GMT. The unmistakable separation between the principal GmtA and CopA signals in this study does not, of course, preclude the presence of CopA in GmtA-containing compartments; it may simply be that the steady-state level of CopA in those compartments is very low compared with that in compartments nearer to the tip.

In most fungi, Golgi cisternae are widely separated, in contrast to the tightly stacked cisternae of animals, plants and the yeast *P. pastoris* (Shorter & Warren, 2002; Mogelsvang *et al.*, 2003) In yeasts, evidence indicates that Golgi cisternae undergo a progressive maturation process, exhibiting different physiological properties and protein contents at different stages of development (Morin-Ganet *et al.*, 2000; Losev *et al.*, 2006; Matsuura-Tokita *et al.*, 2006). On the assumption that CopA and GmtA of *A. nidulans* are indeed Golgi-localized, their non-overlapping distributions can be seen as providing important new evidence that the widely scattered Golgi cisternae of filamentous fungi, like the more ordered cisternae of plants and animals, represent physiologically distinct developmental stages of a single organelle. Recent evidence suggests that Golgi equivalents in *A. nidulans* exhibit net migration towards the growing tip during hyphal growth, at which point mature cisternae may dissipate into secretory vesicles (Hubbard & Kaminskyj, 2008). Presumably this process would be accompanied by large-scale recycling (retrograde transport) of Golgi components for reuse in newly forming cisternae further back in the cell. In keeping with this model, we propose that the GmtA-containing compartments reported in this study may represent early '*cis*-like' cisternae engaged in active biosynthesis, while the more apically located compartments exhibiting high levels of CopA may represent mature '*trans*-like' cisternae, whose high CopA content reflects retrograde transport of materials required for continued production of less mature cisternae. As further evidence for a probable '*trans*-like' nature of the CopA-containing organelles, Hubbard & Kaminskyj (2008) report colocalization of CopA with a transgenic transmembrane fragment of rat α-2,6-sialyltransferase, which in mammals localizes to *trans* Golgi cisternae (Roth *et al.*, 1985).

Now that usable Golgi markers have been introduced (this study; Breakspear *et al.*, 2007), combined with temperature-sensitive mutations in Golgi trafficking (Whittaker *et al.*, 1999; Shi *et al.*, 2004; Yang *et al.*, 2008), significant strides can be made in the study of the structure and function of Golgi equivalents in *A. nidulans* and other filamentous fungi.

ACKNOWLEDGEMENTS

This research was supported by a Research Corporation Cottrell Science Award to L. J.-H., by NSF grant CRUI-0211600 to T. W. H. and D. M. L., by a grant to Rhodes College from the Merck Institute for Higher Education, and by funds from Rhodes College in support of undergraduate research. We thank Mary Miller for the use of her fluorescence microscope and Andrew Breakspear for helpful discussions regarding CopA.

REFERENCES

Abe, M., Noda, Y., Adachi, H. & Yoda, K. (2004). Localization of GDP-mannose transporter in the Golgi requires retrieval to the endoplasmic reticulum depending on its cytoplasmic tail and coatomer. *J Cell Sci* **117**, 5687–5696.

Arakawa, K., Abe, M., Noda, Y., Adachi, H. & Yoda, K. (2006). Molecular cloning and characterization of a *Pichia pastoris* ortholog of the yeast Golgi GDP-mannose transporter gene. *J Gen Appl Microbiol* **52**, 137–145.

Baenziger, J. U. & Fiete, D. (1979). Structural determinants of Concanavalin A specificity for oligosaccharides. *J Biol Chem* **254**, 2400–2407.

Bates, S., Hughes, H. B., Munro, C. A., Thomas, W. P. H., MacCallum, D. M., Bertram, G., Atrih, A., Ferguson, M. A. J., Brown, A. J. P. & other authors (2006). Outer chain *N*-glycans are required for cell wall integrity and virulence of *Candida albicans*. *J Biol Chem* **281**, 90–98.

Berninsone, P. M. & Hirschberg, C. B. (2000). Nucleotide sugar transporters of the Golgi apparatus. *Curr Opin Struct Biol* **10**, 542–547.

Bourett, T. M., James, S. W. & Howard, R. J. (2007). The endomembrane system of the fungal cell. In *The Mycota VIII. Biology of the Fungal Cell*, 1–47. Edited by R. J. Howard & N. A. R. Gow. Berlin: Springer Verlag.

Bowman, S. M. & Free, S. J. (2006). The structure and synthesis of the fungal cell wall. *Bioessays* **28**, 799–808.

Breakspear, A., Langford, K. J., Momany, M. & Assinder, S. J. (2007). CopA : GFP localizes to putative Golgi equivalents in *Aspergillus nidulans*. *FEMS Microbiol Lett* **277**, 90–97.

Cheng, J., Park, T. S., Fischl, A. S. & Ye, X. S. (2001). Cell cycle progression and cell polarity require sphingolipid biosynthesis in *Aspergillus nidulans*. *Mol Cell Biol* **21**, 6198–6209.

Clutterbuck, A. J. & Arst, H. (1995). Genetic nomenclature guide: *Aspergillus nidulans*. *Trends Genet* **11**, 13–14.

Cosson, P. & Letourneur, F. (1997). Coatomer (COPI)-coated vesicles: role in intracellular transport and protein sorting. *Curr Opin Cell Biol* **9**, 484–487.

Cottrell, T. R., Griffith, C. L., Liu, H., Nenninger, A. A. & Doering, T. L. (2007). The pathogenic fungus *Cryptococcus neoformans* expresses two functional GDP–mannose transporters with distinct expression patterns and roles in capsule synthesis. *Eukaryot Cell* **6**, 776–785.

Cullen, P. J., Xu-Friedman, R., Delrow, J. & Sprague, G. F. (2006). Genome-wide analysis of the response to protein glycosylation deficiency in yeast. *FEMS Yeast Res* **6**, 1264–1273.

de Groot, P. W. J., Ruiz, C., Vázquez de Aldana, C. R., Dueñas, E., Cid, V. J., Del Rey, F., Rodríquez-Peña, J. M., Pérez, P., Andel, A. & other authors (2001). A genomic approach for the identification and classification of genes involved in cell wall formation and its regulation in *Saccharomyces cerevisiae*. *Comp Funct Genomics* **2**, 124–142.

De Groot, P. W., Ram, A. F. & Klis, F. M. (2005). Features and functions of covalently linked proteins in fungal cell walls. *Fungal Genet Biol* **42**, 657–675.

De Nobel, J. G., Klis, F. M., Munnik, T., Priem, J. & van den Ende, H. (1990). An assay of relative cell wall porosity in *Saccharomyces cerevisiae*, *Kluyveromyces lactis* and *Schizosaccharomyces pombe*. *Yeast* **6**, 483–490.

Dean, N. (1999). Asparagine-linked glycosylation in the yeast Golgi. *Biochim Biophys Acta* **1426**, 309–322.

Dean, N., Zhang, Y. B. & Poster, J. B. (1997). The *VRG4* gene is required for GDP-mannose transport into the lumen of the Golgi in the yeast, *Saccharomyces cerevisiae*. *J Biol Chem* **272**, 31908–31914.

Galagan, J. E., Calvo, S. E., Cuomo, C., Ma, L. J., Wortman, J. R., Batzoglou, S., Lee, S. I., Bastürkmen, M., Spevak, C. C. & other authors (2005). Sequencing of *Aspergillus nidulans* and comparative analysis with *A. fumigatus* and *A. oryzae*. *Nature* **438**, 1105–1115.

Gao, X.-D. & Dean, N. (2000). Distinct protein domains of the yeast Golgi GDP-mannose transporter mediate oligomer assembly and export from the endoplasmic reticulum. *J Biol Chem* **275**, 17718–17727.

Gao, X.-D., Nishikawa, A. & Dean, N. (2001). Identification of a conserved motif in the yeast Golgi GDP–mannose transporter required for binding to nucleotide sugar. *J Biol Chem* **276**, 4424–4432.

Gemmill, T. R. & Trimble, R. B. (1999). Overview of *N*- and *O*-linked oligosaccharide structures found in various yeast species. *Biochim Biophys Acta* **1426**, 227–237.

Goto, M. (2007). Protein *O*-glycosylation in fungi: diverse structures and multiple functions. *Biosci Biotechnol Biochem* **71**, 1415–1427.

Griffiths, G., Pepperkok, R., Locker, J. K. & Kreis, T. E. (1995). Immunocytochemical localization of β-COP to the ER-Golgi boundary and the TGN. *J Cell Sci* **108**, 2839–2856.

Harris, S. D., Morrell, J. L. & Hamer, J. E. (1994). Identification and characterization of *Aspergillus nidulans* mutants defective in cytokinesis. *Genetics* **136**, 517–532.

Harris, S. D., Read, N. D., Roberson, R. W., Shaw, B., Seiler, S., Plamann, M. & Momany, M. (2005). Polarisome meets Spitzenkörper: microscopy, genetics, and genomics converge. *Eukaryot Cell* **4**, 225–229.

Hill, T. W. & Kafer, E. (2001). Improved protocols for *Aspergillus* minimal medium: trace element and minimal medium salt stock solutions. *Fungal Genet Newsl* **48**, 20–21.

Hill, T. W., Loprete, D. M., Momany, M., Ha, Y., Harsch, L. M., Livesay, J. A., Mirchandani, A., Murdock, J. J., Vaughan, M. J. & Watt, M. B. (2006). Isolation of cell wall mutants in *Aspergillus nidulans* by screening for hypersensitivity to Calcofluor White. *Mycologia* **98**, 399–409.

Howard, R. J. (1981). Ultrastructural analysis of hyphal tip cell growth in fungi: Spitzenkörper, cytoskeleton and endomembranes after freeze-substitution. *J Cell Sci* **48**, 89–103.

Hubbard, M. A. & Kaminskyj, S. G. W. (2008). Rapid tip-directed movement of Golgi equivalents in growing *Aspergillus nidulans* hyphae suggests a mechanism for delivery of growth-related materials. *Microbiology* **154**, 1544–1553.

Ichinomiya, M., Motoyama, T., Fujiwara, M., Takagi, M., Horiuchi, H. & Ohta, A. (2002). Repression of *chsB* expression reveals the functional importance of class IV chitin synthase gene *chsD* in hyphal growth and conidiation of *Aspergillus nidulans*. *Microbiology* **148**, 1335–1347.

Kafer, E. (1977). Meiotic and mitotic recombination in *Aspergillus* and its chromosomal aberrations. *Adv Genet* **19**, 33–131.

Kaminskyj, S. G. (2000). Septum position is marked at the tip of *Aspergillus nidulans* hyphae. *Fungal Genet Biol* **31**, 105–113.

Lesage, G. & Bussey, H. (2006). Cell wall assembly in *Saccharomyces cerevisiae*. *Microbiol Mol Biol Rev* **70**, 317–343.

Losev, E., Reinke, C. A., Jellen, J., Strongin, D. E., Bevis, B. J. & Glick, B. S. (2006). Golgi maturation visualized in living yeast. *Nature* **441**, 1002–1006.

Maertens, J. A. & Boogaerts, M. A. (2000). Fungal cell wall inhibitors: emphasis on clinical aspects. *Curr Pharm Des* **6**, 225–239.

Mansour, M. K. & Levitz, S. M. (2003). Fungal mannoproteins: the sweet path to immunodominance. *ASM News* **69**, 595–600.

Matsuura-Tokita, K., Takeuchi, M., Ichihara, A., Mikuriya, K. & Nakano, A. (2006). Live imaging of yeast Golgi cisternal maturation. *Nature* **441**, 1007–1010.

McCluskey, K. (2003). The Fungal Genetics Stock Center: from Molds to Molecules. In *Advances in Applied Microbiology*, vol. 52, pp. 246–262. Edited by A. Laskin J. Bennett. & G. Gadd. New York: Elsevier.

Mellado, E., Dubreucq, G., Mol, P., Sarfati, J., Paris, S., Diaquin, M., Holden, D. W., Rodriguez-Tudela, J. L. & Latgé, J. P. (2003). Cell wall biogenesis in a double chitin synthase mutant (*chsG* $^{-}$/*chsE*$^{-}$) of *Aspergillus fumigatus*. *Fungal Genet Biol* **38**, 98–109.

Mogelsvang, S., Gomez-Ospina, N., Soderholm, J., Glick, B. S. & Staehelin, L. A. (2003). Tomographic evidence for continuous turnover of Golgi cisternae in *Pichia pastoris*. *Mol Biol Cell* **14**, 2277–2291.

Momany, M., Westfall, P. J. & Abramowsky, G. (1999). *Aspergillus nidulans swo* mutants show defects in polarity establishment, polarity maintenance and hyphal morphogenesis. *Genetics* **151**, 557–567.

Mondésert, G., Clarke, D. J. & Reed, S. I. (1997). Identification of genes controlling growth polarity in the budding yeast *Saccharomyces cerevisiae*: a possible role of *N*-glycosylation and involvement of the exocyst complex. *Genetics* **147**, 421–494.

Morin-Ganet, M. N., Rambourg, A., Deitz, S. B., Franzusoff, A. & Képès, F. (2000). Morphogenesis and dynamics of the yeast Golgi apparatus. *Traffic* **1**, 56–68.

Nayak, T., Szewczyk, E., Oakley, C. E., Osmani, A., Ukil, L., Murray, S. L., Hynes, M. J., Osmani, S. A. & Oakley, B. R. (2006). A versatile and efficient gene-targeting system for *Aspergillus nidulans*. *Genetics* **172**, 1557–1566.

Nishikawa, A., Poster, J. B., Jigami, Y. & Dean, N. (2002). Molecular and phenotypic analysis of *CaVRG4*, encoding an essential Golgi apparatus GDP-mannose transporter. *J Bacteriol* **184**, 29–42.

Oka, T., Hamaguchi, T., Sameshima, Y., Goto, M. & Furukawa, K. (2004). Molecular characterization of protein *O*-mannosyltransferase and its involvement in cell-wall synthesis in *Aspergillus nidulans*. *Microbiology* **150**, 1973–1982.

Osherov, N., Mathew, J. & May, G. S. (2000). Polarity-defective mutants of *Aspergillus nidulans*. *Fungal Genet Biol* **31**, 181–188.

Osmani, A. H., Oakley, B. R. & Osmani, S. A. (2006). Identification and analysis of essential *Aspergillus nidulans* genes using the heterokaryon rescue technique. *Nat Protoc* **1**, 2517–2526.

Philip, B. & Levin, D. E. (2001). Wsc1 and Mid2 are cell surface sensors for cell wall integrity signaling that act through Rom2, a guanine nucleotide exchange factor for Rho1. *Mol Cell Biol* **21**, 271–280.

Protchenko, O., Ferea, T., Rashford, J., Tiedeman, J., Brown, P. O., Botstein, D. & Philpott, C. C. (2001). Three cell wall mannoproteins facilitate the uptake of iron in *Saccharomyces cerevisiae*. *J Biol Chem* **276**, 49244–49250.

Richard, M. L. & Plaine, A. (2007). Comprehensive analysis of glycosylphosphatidylinositol-anchored proteins in *Candida albicans*. *Eukaryot Cell* **6**, 119–133.

Roth, J., Taatjes, D. J., Lucocq, J. M., Weinstein, J. & Paulson, J. C. (1985). Demonstration of an extensive *trans*-tubular network continuous with the Golgi apparatus stack that may function in glycosylation. *Cell* **43**, 287–295.

Shaw, B. D. & Momany, M. (2002). *Aspergillus nidulans* polarity mutant *swoA* is complemented by protein *O*-mannosyltransferase *pmtA*. *Fungal Genet Biol* **37**, 263–270.

Shaw, B. D., Momany, C. & Momany, M. (2002). *Aspergillus nidulans swoF* encodes an *N*-myristoyl transferase. *Eukaryot Cell* **1**, 241–248.

Shi, X., Sha, Y. & Kaminskyj, S. (2004). *Aspergillus nidulans hypA* regulates morphogenesis through the secretion pathway. *Fungal Genet Biol* **41**, 75–88.

Shorter, J. & Warren, G. (2002). Golgi architecture and inheritance. *Annu Rev Cell Dev Biol* **18**, 379–420.

Smith, D. J. & Payton, M. A. (1994). Hyphal tip extension in *Aspergillus nidulans* requires the *manA* gene, which encodes phosphomannose isomerase. *Mol Cell Biol* **14**, 6030–6038.

Szewczyk, E., Nayak, T., Oakley, C. E., Edgerton, H., Xiong, Y., Taheri-Talesh, N., Osmani, S. A. & Oakley, B. R. (2006). Fusion PCR and gene targeting in *Aspergillus nidulans*. *Nat Protoc* **1**, 3111–3120.

Timpel, C., Strahl-Bolsinger, S., Ziegelbauer, K. & Ernst, J. F. (1998). Multiple functions of Pmt1p-mediated protein *O*-mannosylation in the fungal pathogen *Candida albicans*. *J Biol Chem* **273**, 20837–20846.

Turner, G. & Harris, S. D. (1999). Genetic control of polarized growth and branching in filamentous fungi. In *The Fungal Colony* (British Mycological Society Symposia no. 21), 229–260. Edited by N. A. R. Gow, G. D. Robson & G. M. Gadd. Cambridge: Cambridge University Press.

Turner, M. S., Drew, R. H. & Perfect, J. R. (2006). Emerging echinocandins for treatment of invasive fungal infections. *Expert Opin Emerg Drugs* **11**, 231–250.

Upadhyay, S. & Shaw, B. D. (2006). A phosphoglucose isomerase mutant in *Aspergillus nidulans* is defective in hyphal polarity and conidiation. *Fungal Genet Biol* **43**, 739–751.

van der Vaart, J. M., Caro, L. H., Chapman, J. W., Klis, F. M. & Verrips, C. T. (1995). Identification of three mannoproteins in the cell wall of *Saccharomyces cerevisiae*. *J Bacteriol* **177**, 3104–3110.

Verstrepen, K. J., Reynolds, T. B. & Fink, G. R. (2004). Origins of variation in the fungal cell surface. *Nat Rev Microbiol* **2**, 533–540.

Whittaker, S. L., Lunness, P., Milward, K. J., Doonan, J. H. & Assinder, S. J. (1999). sod^{VI}C is an α-COP-related gene which is essential for establishing and maintaining polarized growth in *Aspergillus nidulans*. *Fungal Genet Biol* **26**, 236–252.

Willer, T., Brandl, M., Sipiczki, M. & Strahl, S. (2005). Protein *O*-mannosylation is crucial for cell wall integrity, septation and viability in fission yeast. *Mol Microbiol* **57**, 156–170.

Yang, L., Ukil, L., Osmani, A., Nahm, F., Davies, J., De Souza, C. P., Dou, X., Perez-Balaguer, A. & Osmani, S. A. (2004). Rapid production of gene replacement constructs and generation of a green fluorescent protein-tagged centromeric marker in *Aspergillus nidulans*. *Eukaryot Cell* **3**, 1359–1362.

Yang, Y., Amira, M., El-Ganiny, A. M., Bray, G. E., Sanders, D. A. R. & Kaminskyj, S. G. W. (2008). *Aspergillus nidulans hypB* encodes a Sec7-domain protein important for hyphal morphogenesis. *Fungal Genet Biol* **45**, 749–759.

Yelton, M. M., Hamer, J. E. & Timberlake, W. E. (1984). Transformation of *Aspergillus nidulans* by using a *trpC* plasmid. *Proc Natl Acad Sci U S A* **81**, 1470–1474.

Edited by: H. A. B. Wösten